Bio-based substrate for flexible electronics - application to a 2.45 GHz wearable patch antenna

Abdelghafour Sid, Pierre-Yves Cresson, Nicolas Joly, Flavie Braud, Tuami Lasri

Materials Today Electronics 5 (2023) 100049

Contents lists available at ScienceDirect

Materials Today Electronics

journal homepage: www.elsevier.com/locate/mtelec

Full Length Article

Bio-based substrate for flexible electronics - application to a 2.45 GHz wearable patch antenna

Abdelghafour Sid[a], Pierre-Yves Cresson[a,b,*], Nicolas Joly[b,c], Flavie Braud[a], Tuami Lasri[a]

[a] Institut d'Electronique, de Microélectronique et de Nanotechnologie, University of Lille, F-59000 Lille, France
[b] Univ. Artois, IUT Béthune, F-62408 Béthune, France
[c] Univ. Artois, UniLaSalle, ULR7519—Unité Transformations & Agro-Ressources, F-62408 Béthune, France

ARTICLE INFO

Keywords:
Bio-based and biocompatible material
Cellulose
Green electronics
Wearable antenna
Flexible RF circuits

ABSTRACT

In this paper, a bio-based and biocompatible polymer, Cellulose Laurate (CL), is proposed for flexible radio-frequency (RF) electronics. The synthesis of CL films together with their characterizations (chemical, thermal, mechanical and dielectric) are presented. The results obtained allow considering this material for RF flexible applications as a possible alternative to petrosourced substrates. Therefore, CL has been used to fabricate a flexible patch antenna that operates in an industrial, scientific and medical (ISM) frequency band. The central frequency selected is 2.45 GHz. The antenna fabrication process is based on the combination of laser structuring and the use of copper adhesive tape. Measurements of the antenna reflection coefficient and radiation patterns show that CL is a good candidate as a RF substrate. Furthermore, it is demonstrated that the antenna performance is only slightly impacted under bending conditions.

1. Introduction

Wearable antennas have attracted a lot of attention in recent years due to the many advantages they provide, like flexibility, lightweight and low cost. They have many applications in the fields of wireless communications and sensors [1].

Depending on the application, different types of substrates are used for the fabrication of antennas. For example, for wearable applications on clothing, textile substrates are interesting because of their ability to be easily integrated into fabrics [2]. Paper-based substrates, widely available and inexpensive, are a good choice for green electronics [2] but are not preferred for wearable applications because of their lack of hydrophobicity. In fact, the most widely used substrates are polymer-based substrates. Among the most commonly used polymers are polyimide (Kapton) [3], polyethylene terephthalate (PET) [4] and polydimethylsiloxane (PDMS) [5].

The major drawback of these materials is that they are obtained from petroleum sources. For this reason, there is growing interest in alternatives that reduce the use of such materials, and thus decrease the dependence on oil and consequently the environmental footprint of electronic devices.

Indeed, there is a growing interest in using biopolymers for RF applications that involve the fabrication of passive [6] and active [7] RF circuits. Biopolymers are promising raw materials to replace conventional polymers in RF applications due to a lot of features such as low weight, low cost, abundance, biocompatibility, biodegradability and mechanical properties [8]. Polysaccharides, in particular Fatty Acid Cellulose Esters (FACEs), have been identified as an interesting solution to switch from petrochemical polymers to natural polymers to produce plastics. Actually, cellulose esters, which have excellent film-forming characteristics, are now well known as commercially important thermoplastic polymers [9]. Furthermore, FACEs, obtained by grafting fatty acid chains onto cellulose backbone, are a well-known class of hydrophobic materials. FACEs can be obtained by cellulose acylation, consisting in the reaction, in homogeneous LiCl/*N,N*-dimethylacetamide reaction media, between fatty acid chlorides and cellulose, in presence of a basic catalyst, the *N,N*-dimethyl-4-aminopyridine (DMAP) [10]. We have selected from this family of FACEs one of the most common, cellulose laurate (CL). It is synthesized using lauroyl chloride as fatty acid derivative and is characterized by its high elasticity and good hydrophobicity compared to the cellulose ester family.

To validate the choice of the selected biopolymer as RF substrate, different kind of characterizations are first performed. Then, a comparison of its characteristics with other polymers widely used in RF flexible electronics applications is proposed.

Finally, a rectangular patch antenna operating at 2.45 GHz, chosen to demonstrate the suitability of this bio-based polymer for flexible RF electronics is investigated. The design and the optimization of the flexible and wearable antenna proposed are performed using ANSYS HFSS software. The fabrication process of the antenna is based on laser struc-

* Corresponding author.
E-mail address: pierre-yves.cresson@univ-lille.fr (P.-Y. Cresson).

https://doi.org/10.1016/j.mtelec.2023.100049
Received 22 February 2023; Received in revised form 5 May 2023; Accepted 19 June 2023

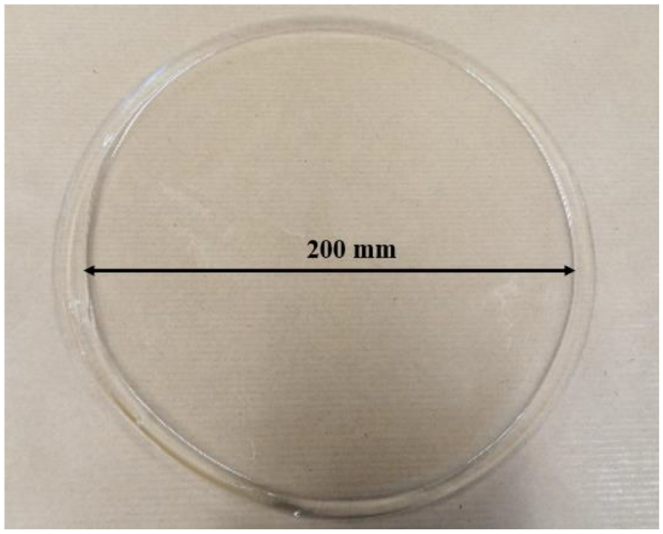

Fig. 1. Cellulose laurate film.

turing and adhesive copper. This process is suitable for green electronics and is potentially compatible with all types of substrates less resistant to high temperatures and chemicals. The antenna characterization ends with the evaluation of its performance under bending conditions and tests on a human body.

2. Material and methods

2.1. Materials

Reagents and solvents were stored at room temperature and used without further purification: microcrystalline cellulose (20 μm, DP = 200, Aldrich); *N, N*-dimethyl-4-aminopyridine (DMAP, 99%, Acros); *N, N*-dimethylacetamide (DMAc, 99%, Acros); anhydrous lithium chloride (99%, Acros); lauroyl chloride (98%, Aldrich); chloroform (≥ 99%, Carlo Erba); methanol (≥ 99%, Carlo Erba). Deuterated chloroform (Aldrich) used for NMR analysis was stored at 4°C.

2.2. Synthesis of cellulose laurate

200 mL of a 30 g.L^{-1} cellulosic solution, consisting in pre-treated cellulose in a 6.7% LiCl/DMAc (v/w) system [11] (6 g of cellulose; 37 mmol of anhydroglucose unit, 1 equiv.) and DMAP (13,5 g; 111 mmol; 3 equiv.) were stirred at 80°C until complete solubilization. Fatty acyl chloride (77 mL, 9 equiv. per anhydroglucose unit) was then added and reaction medium was stirred at 80°C during 3 hours. The reaction media was poured into methanol (3 vol) and the precipitated cellulose trilaurate (CL) was purified by a repeated solubilization/precipitation process using chloroform and methanol, respectively. CL was finally dried in air at room temperature.

CL, obtained as a cotton-like solid, was converted into film material by casting in chloroform in a 20 cm diameter glass Petri dish (10 g to 20 g of CL in 150 to 300 mL of chloroform according to the desired material thickness), leading to a translucent film after complete chloroform evaporation.

The films thus obtained (Fig. 1) are then characterized for their chemical structure and properties.

2.3. Chemical Characterization

The film of CL has been characterized by Fourier Transformed InfraRed (FTIR) spectroscopy using an Agilent Cary630 apparatus equipped with an ATR accessory. ^{1}H-NMR spectroscopy was performed after dissolution of CL (10 mg) in deuterated chloroform using a Bruker DRX-300 Spectrometer (operating at 300 MHz). ^{1}H-NMR spectroscopy allowed us to determine CL purity and confirmed that the number of fatty chains linked per anhydroglucose unit (DS) is equal to 3 (maximum value), using an integration method already described in literature [12].

2.4. Thermal Characterization

Differential Scanning Calorimetry analyses were carried out on a TA Instruments DSC Q20 apparatus, calibrated using high purity indium samples, to determine thermal transitions in CL. About 10 mg of CL film sample was heated and then cooled, cycle experiments conducted at 20°C.min^{-1} under nitrogen atmosphere. Thermal degradation was measured using TA Instruments Discovery SDT650. About 30 mg of CL was heated under nitrogen atmosphere from 40°C to 700°C at 20°C.min^{-1} and the weight loss was recorded according to temperature.

2.5. Mechanical behavior and dynamic mechanical analysis (DMA)

Mechanical behavior was studied in uniaxial tensile mode using a Shimadzu Autograph AGS-X apparatus. Tensile tests were conducted at room temperature, at a constant crosshead speed of 5 mm.min^{-1}, and samples were cut out from the CL solvent-cast films as dumbbell shape samples.

2.6. Contact Angle Measurements

Contact angle measurements were carried out with a water drop of 3 μL, at ambient humidity and room temperature, using an Apollo Instruments OCA 20 contact angle apparatus operating with the sessile drop method. Contact angles were measured on both sides of the drop by the ellipse-fitting calculation method, at a drop age of 10 seconds. Ten values, at least, were averaged.

2.7. Dielectric microwave characterization

The knowledge of the CL dielectric properties (permittivity ε_r, and loss tangent tanδ) is mandatory for the design of microwave circuits. To determine them, a method called “the two-lines method” was used. To that end, the transmission and reflection coefficients of CPW (Coplanar Waveguide) lines fabricated on a 0.4 mm-thick CL substrate were measured using GSG (Ground-Signal-Ground) probes connected to a Vector Network Analyzer (VNA) (Keysight E8361A) [13]. The dielectric properties of CL were extracted from the measured propagation constant associated to a retro simulation procedure using the software ANSYS HFSS.

In the Table 1 and Table 2 are gathered the results of the different characterizations mentioned above.

3. Results

The characteristics of CL were recorded and compared to those of petrochemical materials usually used as substrate for electronics (Table 1).

CL has a contact angle, θ, of 100° and so can be considered as a hydrophobic material ($\theta > 90°$). Compared to other polymers, CL has a good hydrophobicity, a better elasticity and a good elongation at break. Regarding the tensile strength, it is low compared to Kapton or PET, but 12 MPa of tensile strength is enough for wearable applications.

Considering CL thermal properties, they are almost similar to those of other polymers. These properties should be taken into account when CL is used as substrate for active circuits (such as an amplifier) to define the operating point.

It can also be noted that CL presents dielectric properties close to those of polymers which are more classically used for flexible RF electronic devices. In particular, the level of losses makes it competitive. All

Table 1
Comparison of Cellulose Laurate characteristics with those of polymers used in RF.

Material		Kapton	PDMS	PET	PTFE	CL
Hydrophobicity	**Contact angle Measurement (°)**	70[14]	113[15]	80.9 [16]	106.9[17]	100
Mechanical properties	**Young's modulus**	2.62GPa[18]	2.42MPa [19]	3.29GPa [20]	0.59GPa [21]	135MPa
	Elongation at break (%)	82[18]	30-90 [19]	1.6-600[20]	70-600[21]	60-80
	Tensile strength (MPa)	231[18]	4.2[22]	61.8[20]	131[21]	12
Thermal behavior	**Glass transition temperature Tg (°C)**	360 -410[23]	-123[24]	70[25]	129[26]	100-110
	Degradation temperature Td (°C)	500[23]	400[27]	120[28]	536.2 [29]	250
Dielectric properties @ 2.45GHz	ϵ_r	3.5[30]	2.7[31]	2.2[32]	2.2[33]	2.66
	tanδ	0.002[30]	0.04[31]	0.03[32]	0.002[33]	0.025
Green		**No**	**No**	**No**	**No**	**Yes**

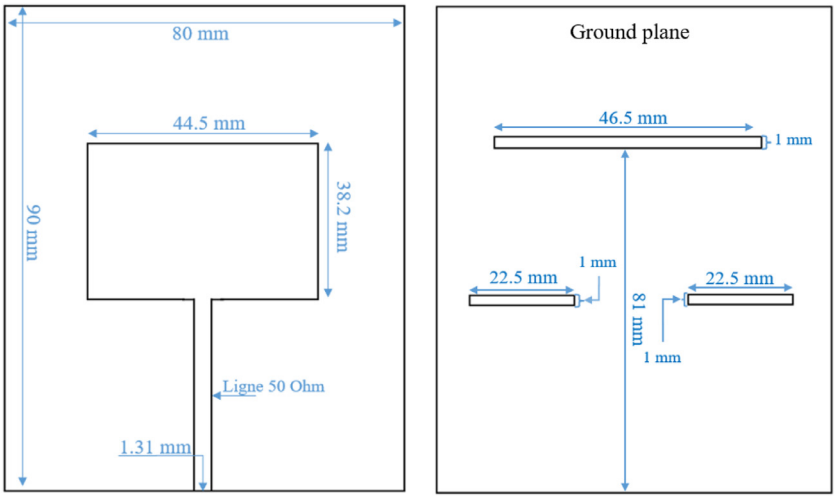

Fig. 2. Antenna topology and dimensions (a) top view (b) bottom view.

together, the characteristics of this bio-based polymer pave the way for a green flexible and wearable RF electronics. And, in particular, its bio-compatibility [34] renders it a good choice for biomedical applications.

We present in the following the exploitation of this material for the fabrication of a flexible and wearable patch antenna.

4. Application

To demonstrate the suitability of this bio-material as a RF substrate, we have designed a device widely used in on-body applications: a patch antenna. In this kind of applications, the device has to be both wearable and flexible.

4.1. Antenna design

The microstrip patch antenna was designed at 2.45 GHz on a 0.4 mm-thick CL substrate. As initial values for the length and the width of the patch antenna, equations given in [35] have been used. Then, to realize an antenna with a good gain, slots are introduced in the ground plane. This technique has already been applied for the improvement of the gain [36,37]. All dimensions of the antenna and the positions of the slots are determined by using the ANSYS HFSS optimization tool to achieve high gain and good matching at 2.45 GHz. All the dimensions of the optimized structure are given in Fig. 2. In Table 2 are given the properties of the various materials constituting the antenna (Fig. 3). The simulation study takes into account all materials, including the adhesive.

In order to better understand the impact of the adhesive layer (h_a, ϵ_{ra}) on the antenna characteristics, a study was performed on ANSYS HFSS. It consists first in varying the thickness of the adhesive layer and observing the antenna gain and resonance frequency (fr).

Fig. 4a illustrates how the effective dielectric constant (ϵ_{eff}) of the structure (Fig. 3) changes with the thickness of the adhesive layer (h_a).

Table 2
Different materials characteristics at 2.45 GHz.

Material	Parameter	Value
Cellulose laurate	ϵ_r	2.66
	tanδ	0.025
	h	400 μm
Copper	σ_{cu}	5.8 10^7 S/m
	h_c	35 μm
Adhesive	ϵ_{ra}	1.2
	h_a	15 μm

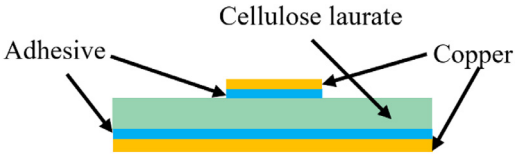

Fig. 3. Stack-up of the proposed antenna.

In this simulation, the properties of the different materials are those given in Table 2. One can note a decrease of the effective dielectric constant as a function of the adhesive layer thickness. This variation of the ϵ_{eff} leads to the increase of the resonance frequency according to h_a (Fig. 4b).

Fig. 5 shows the simulated gain of the antenna as a function of the thickness of the adhesive layer. It can be observed that the gain increases slightly with the adhesive layer thickness. This can be explained by the fact that the adhesive layer brings no additional losses (tanδ=0 for the adhesive).

Fig. 6 presents the impact of the dielectric constant of the adhesive layer on the resonance frequency and the gain. An increase of ϵ_{ra} results

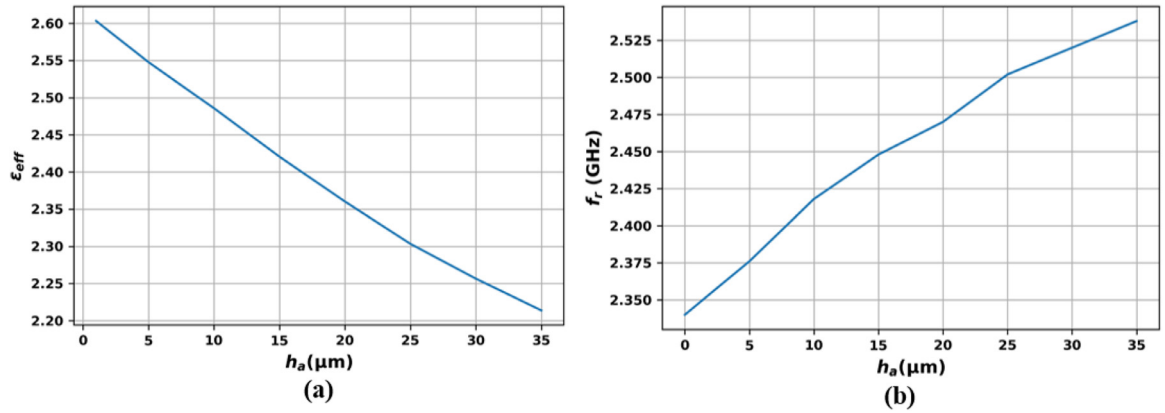

Fig. 4. Simulated effective dielectric constant (a) and antenna resonance frequency (b) versus the adhesive thickness.

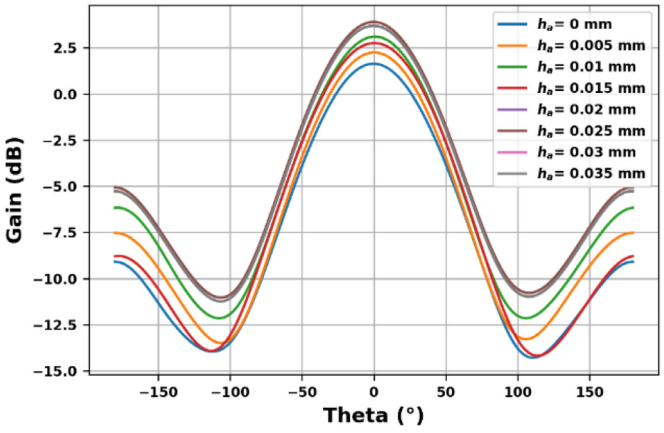

Fig. 5. Simulated gain for different values of the adhesive thickness.

in a rise of the effective permittivity and consequently to a drop of the resonance frequency (Fig. 6a). The impact on the antenna gain is low (Fig. 6b).

4.2. Antenna fabrication

In order to avoid the use of high temperatures and potentially aggressive chemicals for our bio-based material, we have developed a fabrication process that does not involve conventional microelectronics manufacturing methods such as photolithography. This process is characterized, in particular, by the simplicity of implementation and the speed of execution. It is inspired by the technique proposed in [38] and [39] and based on the use of a laser to cut the adhesive copper to the wanted shape and the use of adhesive tape to transfer the desired copper part onto the substrate.

The fabrication process, illustrated in Fig. 7, begins by fixing a piece of adhesive copper on glass using double-sided adhesive tape (Fig. 7a). Then, we use the laser to trace the shape of the circuit on the copper (Fig. 7b). At that point, we use a single-sided adhesive tape to extract the desired copper part (Fig. 7(c and d)). Finally, we transfer this part of copper to the biopolymer and carefully remove the adhesive tape (Fig. 7(e and f)).

Cutting with laser is a precise process that requires the adjustment of a set of parameters (wavelength, power, speed, etc.). These obviously depend on the type of material being cut. Thus, the choice of the set of parameters for copper is made after a series of optimizations; a photograph of the final antenna prototype is given in Fig. 8.

4.3. Antenna characterization

The fabricated antenna was first characterized with a Vector Network Analyzer (N5242A Agilent Technologies) through the measurement of its reflection coefficient. After that, the radiation patterns were measured in an anechoic chamber by using a standard horn antenna (SAS–200/571) and an Agilent 8735ES VNA (30 kHz–6 GHz).

The results obtained are presented in Fig. 9 and Fig. 10 respectively for the reflection coefficient and the radiation patterns. In general, a good agreement is observed between simulations and measurements for the reflection coefficient and radiation patterns. One can note, in partic-

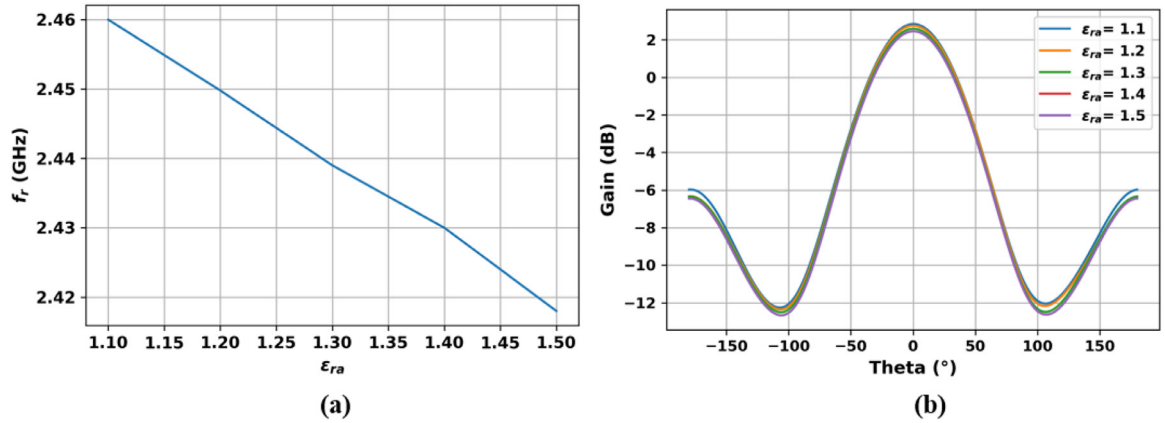

Fig. 6. Simulation of the impact of the adhesive layer dielectric constant on (a) the resonance frequency (b) the gain.

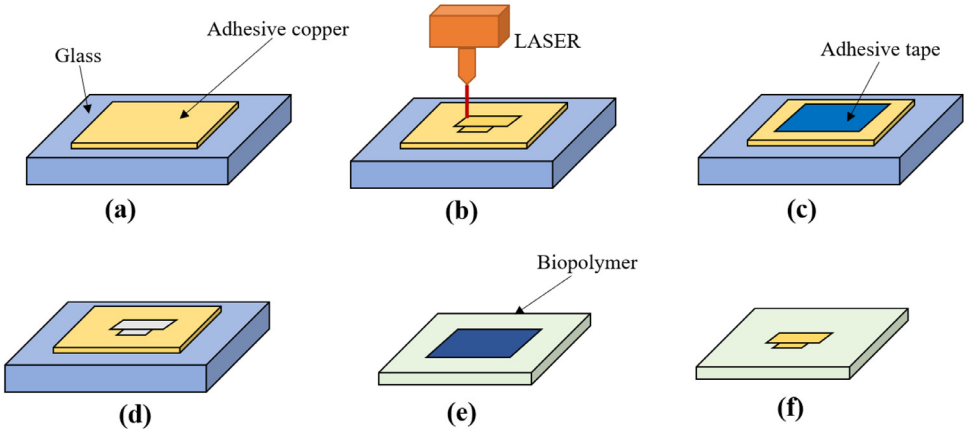

Fig. 7. Main steps for the antenna fabrication.

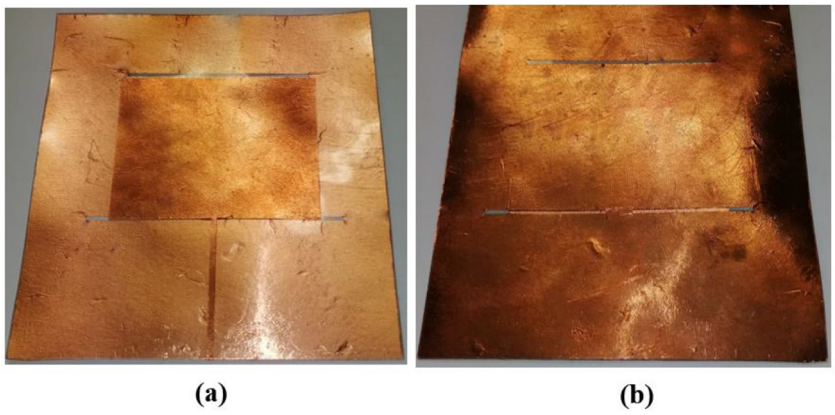

Fig. 8. Antenna prototype (a) top view (b) bottom view.

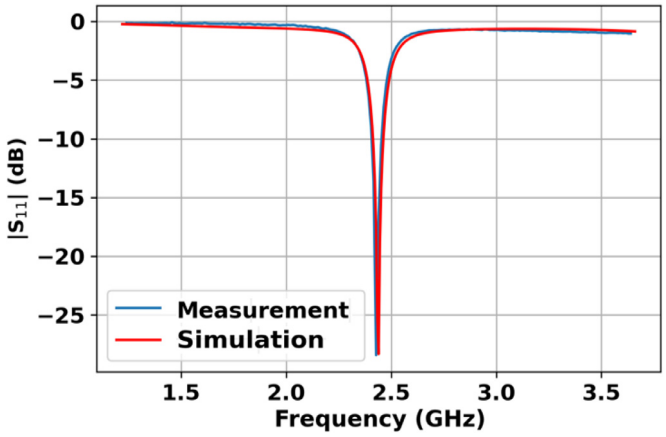

Fig. 9. Simulated and measured antenna reflection coefficients.

ular, that the reflection coefficient is lower than -20 dB at the resonance frequency and that the bandwidth at -10 dB is between 2.41 GHz and 2.47 GHz.

Regarding the radiation patterns, the maximum gain measured for the null angle is equal to 1.9 dBi for the H plane and 1.8 dBi for the E plane. Concerning the aperture angle at 3 dB, it is equal to 75° for the H plane (XZ) and 72° for the E plane (YZ).

The proposed antenna can potentially be used in a situation where it undergoes a bending, so its flexibility must be evaluated. For this, the antenna is characterized by applying several radius of curvature (40 mm, 70 mm and 120 mm) using patterns made in ABS by 3D printing as shown in Fig. 11.a (40 mm is a radius value close to that of a human arm.). A photograph of the antenna bent using the 40 mm radius pattern is shown in Fig. 11b. The comparisons of the measurement results to the simulation data for the reflection coefficient and the radiation diagrams are given in the Fig. 12 and Fig. 13 respectively.

First, a good agreement is observed between the simulation and the measurement. Moreover, the resonance frequency and the maximum gain direction are almost unchanged, while a small decrease in gain and directivity is recorded.

So, these tests demonstrate that the different bending configurations applied to the antenna (Fig. 11) have very little effect on the performance of the proposed antenna.

The impact of mechanical stresses on the adhesiveness of the copper has also been checked. Although the evaluation was conducted in an artisanal manner (series of manual bending tests), the adhesive was shown to have excellent adhesive properties, allowing the copper to remain attached to the substrate. It is worth mentioning that adhesive copper is widely used for RF applications, especially in case of paper substrates. Examples of applications can be found in the literature such as a 24 GHz radar front-end [40], a patch antenna array [41] and a mixer [42].

4.4. SAR evaluation and on-body tests

As the different tests show good performance of the antenna made on CL substrate even in bending situations, its use for wearable applications can be considered. Nevertheless, before evaluating the stability of the antenna performance on a human body, we first ensure compliance with safety regulations. For this purpose, the specific absorption rate (SAR),

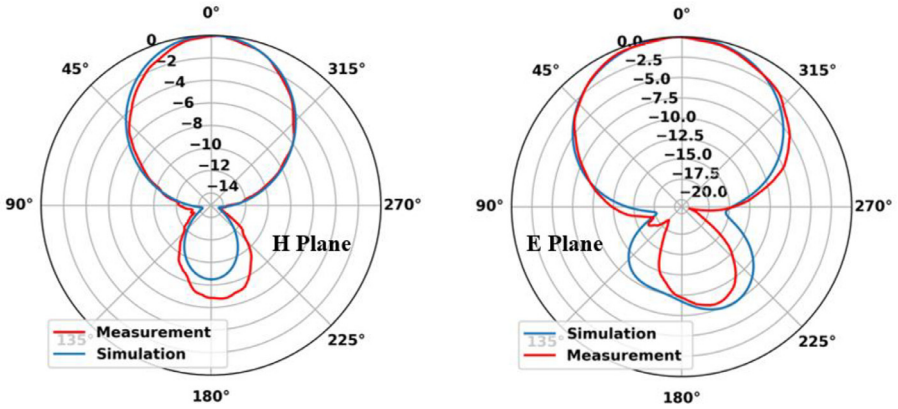

Fig. 10. Simulated and measured far-field antenna radiation patterns in the H and E planes.

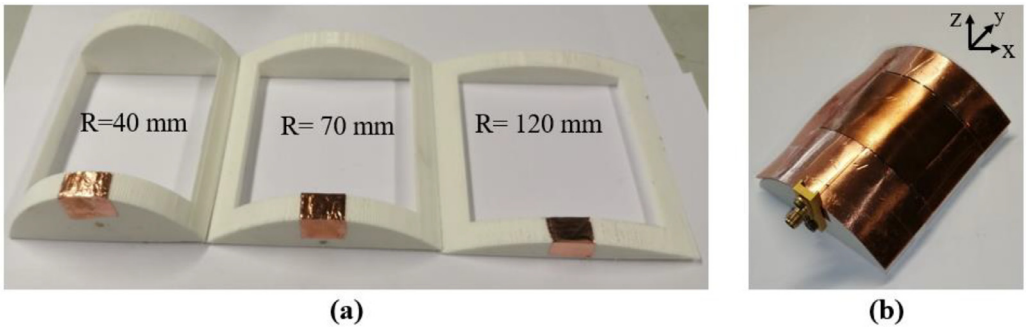

Fig. 11. (a) Three bending radii (b) Bended antenna (R=40 mm).

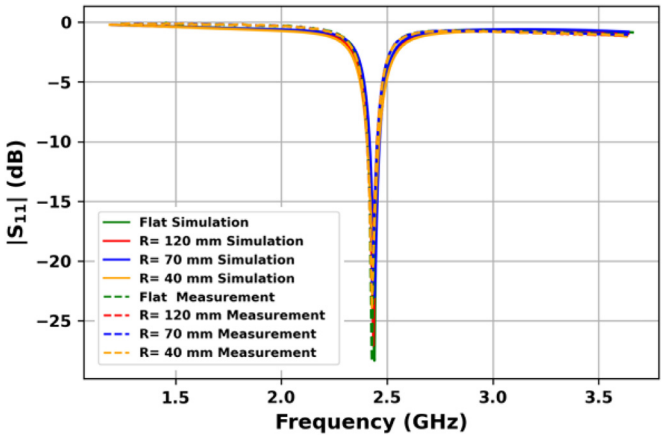

Fig. 12. Simulated and measured reflection coefficients for different bending radii (40, 70 and 120 mm) applied to the antenna.

which is the power absorbed by the human body, is estimated. It must be less than the limit of 1.6 W/kg under 1 g of tissue for US standards, and less than the limit of 2 W/kg under 10 g of tissue for European standards.

The average SAR was simulated on a single homogeneous layer of tissue modeled in the ANSYS HFSS library (1048 kg/m^3 density), for 1 g and 10 g of tissue. The input power is 1 W and the distance between the model (human tissue) and the antenna ground plane is equal to 0.5 mm (Fig. 14).

Simulations show that the maximum SAR values at 2.45 GHz are 0.1298 W/kg under 1 g of tissue and 0.0335 W/kg under 10 g of tissue. So, the maximum SAR values are well below the limits required by international standards.

After the check of the conformity to the safety regulations of the proposed CL-supported antenna, we have tested the antenna on a human body. To that end, the antenna was placed on a real subject, for different positions on the body (arm, chest and back) (Fig. 15).

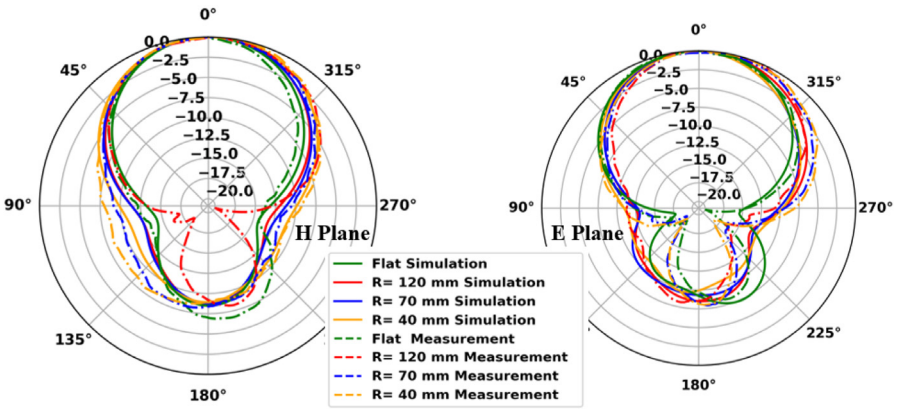

Fig. 13. Simulated and measured far-field radiation patterns of the antenna for different bending radii (40, 70 and 120 mm) applied to the antenna.

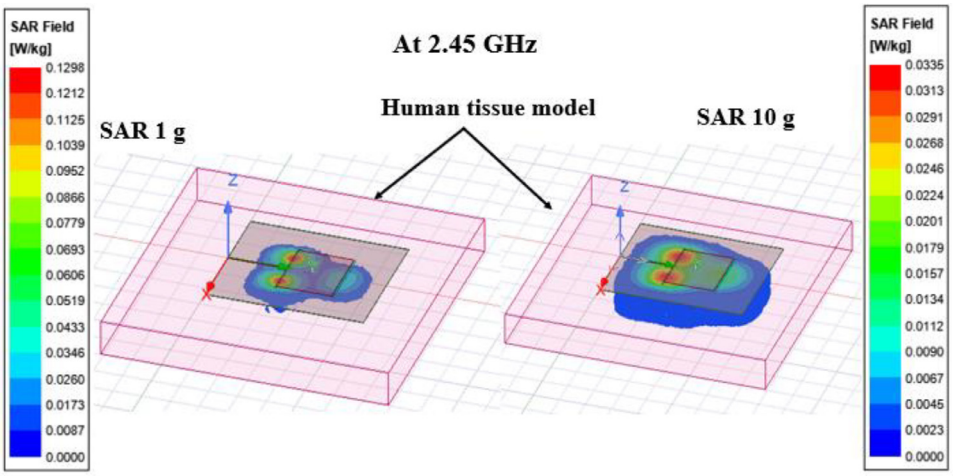

Fig. 14. Simulated SAR at 2.45 GHz of the proposed antenna for 1 g and 10 g of tissue.

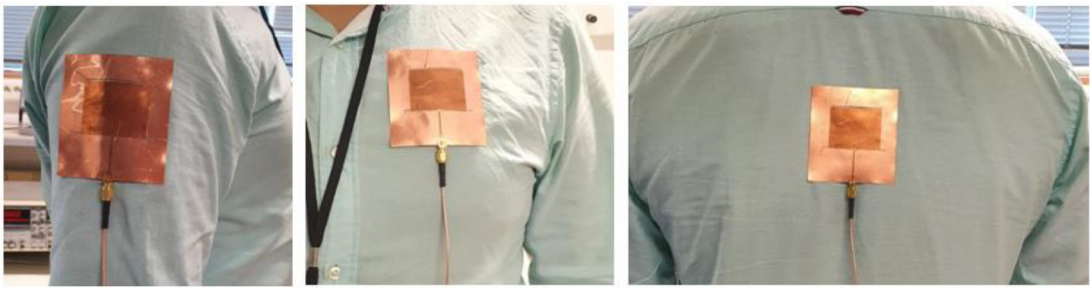

Fig. 15. Antenna at different positions on a human body.

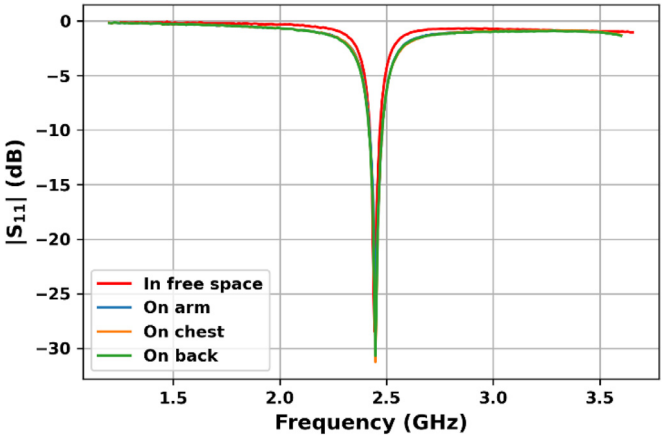

Fig. 16. Reflection coefficient measured in free space and at different positions on the human body.

According to the reflection coefficient measurements shown in Fig. 16, no significant degradation of the antenna performance is observed when it is placed on the human body, whatever the position.

It is worth mentioning that in a previous study a dual-band antenna, also using a CL substrate, has been fabricated by means of an alternative method [43]. Compared to this latter, the antenna proposed in this paper is better in terms of stability. Indeed, whether under bending conditions or when placed on a human body, it shows a better steadiness than the previous antenna that suffers from a resonance frequency shift and shows a weaker matching when placed on a human body. Additionally, it has a lower SAR value, making it safer. Finally, this antenna, compared to the previous one, permits the reduction of the back radiation that is desirable for WBAN applications.

5. Conclusion

In this work, a bio-based substrate, cellulose laurate (CL), is proposed to replace conventional polymers for flexible electronics applications. The different characterizations achieved demonstrate that CL was potentially usable as RF substrate. In particular, its dielectric and mechanical characteristics suggested that RF applications where mechanical flexibility is required could be addressed.

Therefore, CL substrate was used for the fabrication of a slotted microstrip patch antenna using a process based on adhesive copper tape and laser structuring. The different investigations performed demonstrate a good agreement between the simulations and the measurements for the reflection coefficient and the radiation patterns of the patch antenna. Finally, tests under different bending configurations and on a human body show only a slight performance degradation, which makes our solution suitable for flexible and wearable applications. In addition to its flexibility, its biocompatibility makes the CL suitable for WBAN (Wireless Body Area Networks) applications in healthcare and sport, for example.

All together, the results obtained demonstrate that the proposed bio-based polymer is an interesting candidate for the development of flexible and green electronics.

Declaration of Competing Interest

The authors declare that they have no known competing financial interests or personal relationships that could have appeared to influence the work reported in this paper.

Data availability

The authors are unable or have chosen not to specify which data has been used.

References

[1] K.N. Paracha, S.K. Abdul Rahim, P.J. Soh, M. Khalily, Wearable Antennas: A Review of Materials, Structures, and Innovative Features for Autonomous Communication and Sensing, IEEE Access 7 (2019) 56694–56712, doi:10.1109/ACCESS.2019.2909146.

[2] Joao Vicente Faria, Flexible Antennas Design and Test for Human Body Applications Scenarios, Instituto Superior Técnico, Lisboa, Portugal, 2015.

[3] I. Ibanez Labiano, A. Alomainy, Flexible inkjet-printed graphene antenna on Kapton, Flex. Print. Electron. 6 (2) (Jun. 2021) 025010, doi:10.1088/2058-8585/ac0ac1.

[4] G. Tomaszewski, P. Jankowski-Mihułowicz, J. Potencki, A. Pietrikova, P. Lukacs, Inkjet-printed HF antenna made on PET substrate, Microelectron. Reliab. 129 (Feb. 2022) 114473, doi:10.1016/j.microrel.2021.114473.

[5] D.K. Janapala, M. Nesasudha, T.M. Neebha, R. Kumar, Flexible PDMS Antenna Backed with Metasurface for 2.4GHz Wearable Applications, in: 2019 IEEE 1st International Conference on Energy, Systems and Information Processing (ICESIP), IEEE, Chennai, India, Jul. 2019, pp. 1–3, doi:10.1109/ICESIP46348.2019.8938235.

[6] A. Sid, P. Cresson, N. Joly, F. Braud, B. Genestie, T. Lasri, 2.45 GHz natural polymer-based flexible bandpass filter exploiting laser structuring, Microw. Opt. Technol. Lett. 64 (4) (Sep. 2021) 727–732, doi:10.1002/mop.33194.

[7] H. Zhang, et al., Heterogeneously integrated flexible microwave amplifiers on a cellulose nanofibril substrate, Nat. Commun. 11 (1) (Dec. 2020) Art. no. 1, doi:10.1038/s41467-020-16957-4.

[8] P.Y. Cresson, G. Boussatour, S. Li, B. Genestie, N. Joly, T. Lasri, Wideband (10–67 GHz) Dielectric Properties of Biosourced Cellulose Ester Flexible Films, IEEE Trans. Microw. Theory Tech. 68 (6) (Jun. 2020) Art. no. 6, doi:10.1109/TMTT.2020.2985653.

[9] K.J. Edgar, et al., Advances in cellulose ester performance and application, Prog. Polym. Sci. 26 (9) (Nov. 2001) Art. no. 9, doi:10.1016/S0079-6700(01)00027-2.

[10] L. Crépy, V. Miri, N. Joly, P. Martin, J.M. Lefebvre, Effect of side chain length on structure and thermomechanical properties of fully substituted cellulose fatty esters, Carbohydr. Polym. 83 (4) (Feb. 2011) Art. no. 4, doi:10.1016/j.carbpol.2010.10.045.

[11] L. Duchatel-Crépy, et al., Substitution degree and fatty chain length influence on structure and properties of fatty acid cellulose esters, Carbohydr. Polym. 234 (Apr. 2020) 115912, doi:10.1016/j.carbpol.2020.115912.

[12] N. Joly, R. Granet, P. Branland, B. Verneuil, P. Krausz, New methods for acylation of pure and sawdust-extracted cellulose by fatty acid derivatives—Thermal and mechanical analyses of cellulose-based plastic films, J. Appl. Polym. Sci. 97 (3) (Aug. 2005) 1266–1278, doi:10.1002/app.21783.

[13] G. Boussatour, P.Y. Cresson, B. Genestie, N. Joly, T. Lasri, Dielectric Characterization of Polylactic Acid Substrate in the Frequency Band 0.5–67 GHz, IEEE Microw. Wirel. Compon. Lett. 28 (5) (May 2018) Art. no. 5, doi:10.1109/LMWC.2018.2812642.

[14] H. Kizil, M.O. Pehlivaner, L. Trabzon, Surface Plasma Characterization of Polyimide Films for Flexible Electronics, Adv. Mater. Res. 970 (Jun. 2014) 132–135, doi:10.4028/www.scientific.net/AMR.970.132.

[15] A. Mata, A.J. Fleischman, S. Roy, Characterization of Polydimethylsiloxane (PDMS) Properties for Biomedical Micro/Nanosystems, Biomed. Microdevices 7 (4) (Dec. 2005) 281–293, doi:10.1007/s10544-005-6070-2.

[16] T. Homola, L.Y.L. Wu, M. Černák, Atmospheric Plasma Surface Activation of Poly(Ethylene Terephthalate) Film for Roll-To-Roll Application of Transparent Conductive Coating, J. Adhes. 90 (4) (Apr. 2014) 296–309, doi:10.1080/00218464.2013.794110.

[17] J. Włoch, A.P. Terzyk, M. Wiśniewski, P. Kowalczyk, Nanoscale Water Contact Angle on Polytetrafluoroethylene Surfaces Characterized by Molecular Dynamics–Atomic Force Microscopy Imaging, Langmuir 34 (15) (Apr. 2018) 4526–4534, doi:10.1021/acs.langmuir.8b00257.

[18] L. Baxter et al., "Thermoplastic micro- and nanocomposites for neutron shielding," in Micro and Nanostructured Composite Materials for Neutron Shielding Applications, Elsevier, 2020, pp. 53–82. doi:10.1016/B978-0-12-819459-1.00003-9.

[19] K. Song, N.K. Cho, K. Park, C.S. Kim, Investigating Mechanical Behaviours of PDMS Films under Cyclic Loading, Polymers 14 (12) (Jun. 2022) 2373, doi:10.3390/polym14122373.

[20] "MatWeb - Material Property Data (PET)." [Online]. Available: https://www.matweb.com/search/DataSheet.aspx?MatGUID=a696bdcdff6f41dd98f8eec3599eaa20

[21] "MatWeb - Material Property Data (Overview of materials for Polytetrafluoroethylene (PTFE))." [Online]. Available: https://www.matweb.com/search/DataSheet.aspx?MatGUID=4e0b2e88eeba4aaeb18e8820f1444cdb&ckck=1

[22] R. Ariati, F. Sales, A. Souza, R.A. Lima, J. Ribeiro, Polydimethylsiloxane Composites Characterization and Its Applications: A Review, Polymers 13 (23) (Dec. 2021) 4258, doi:10.3390/polym13234258.

[23] "DuPontTM Kapton® Polyimide Film Products of Decomposition." [Online]. Available: https://www.dupont.com/content/dam/dupont/amer/us/en/products/ei-transformation/documents/EI-10142_Kapton-Summary-of-Properties.pdf

[24] K. Zalewski, Z. Chyłek, W.A. Trzciński, A Review of Polysiloxanes in Terms of Their Application in Explosives, Polymers 13 (7) (Mar. 2021) 1080, doi:10.3390/polym13071080.

[25] , Specialized analytical methods in plasticizer testing, in: Handbook of Plasticizers, Elsevier, 2012, pp. 563–571, doi:10.1016/B978-1-895198-50-8.50017-5.

[26] Y. Kaplan, Role of Reinforcement Materials on Mechanical and Tribological Properties of PTFE Composites, Polym. Korea 44 (4) (Jul. 2020) 436–444, doi:10.7317/pk.2020.44.4.436.

[27] G. Camino, S.M. Lomakin, M. Lazzari, Polydimethylsiloxane thermal degradation Part 1. Kinetic aspects, Polymer 42 (6) (Mar. 2001) 2395–2402, doi:10.1016/S0032-3861(00)00652-2.

[28] R. Panowicz, et al., Properties of Polyethylene Terephthalate (PET) after Thermo-Oxidative Aging, Materials 14 (14) (Jul. 2021) 3833, doi:10.3390/ma14143833.

[29] V. Henri, E. Dantras, C. Lacabanne, A. Dieudonne, F. Koliatene, Thermal ageing of PTFE in the melted state: Influence of interdiffusion on the physicochemical structure, Polym. Degrad. Stab. 171 (Jan. 2020) 109053, doi:10.1016/j.polymdegradstab.2019.109053.

[30] S. Ahmed, F.A. Tahir, A. Shamim, H.M. Cheema, A Compact Kapton-Based Inkjet-Printed Multiband Antenna for Flexible Wireless Devices, IEEE Antennas Wirel. Propag. Lett. 14 (2015) 1802–1805, doi:10.1109/LAWP.2015.2424681.

[31] P.Y. Cresson, et al., 1 to 220 GHz Complex Permittivity Behavior of Flexible Polydimethylsiloxane Substrate, IEEE Microw. Wirel. Compon. Lett. 24 (4) (Apr. 2014) Art. no. 4, doi:10.1109/LMWC.2013.2295230.

[32] X. Guo, Y. Hang, Z. Xie, C. Wu, L. Gao, C. Liu, Flexible and wearable 2.45 GHz CPW-fed antenna using inkjet-printing of silver nanoparticles on pet substrate, Microw. Opt. Technol. Lett. 59 (1) (Jan. 2017) 204–208, doi:10.1002/mop.30261.

[33] W. Su, J. Zhu, H. Liao, M.M. Tentzeris, Wearable Antennas for Cross-Body Communication and Human Activity Recognition, IEEE Access 8 (2020) 58575–58584, doi:10.1109/ACCESS.2020.2982965.

[34] L. Crépy, et al., Evaluation of a bio-based hydrophobic cellulose laurate film as biomaterial-Study on biodegradation and cytocompatibility, J. Biomed. Mater. Res. B Appl. Biomater. 100B (4) (May 2012) 1000–1008, doi:10.1002/jbm.b.32665.

[35] C.A. Balanis, Antenna theory: analysis and design, 3rd ed., John Wiley, Hoboken, NJ, 2005.

[36] A. Talukder, E. Islam, Design and Simulation Study of E Shaped Slotted Microstrip Patch Antenna by HFSS for 5G applications, in: 2021 IEEE International Symposium on Antennas and Propagation and USNC-URSI Radio Science Meeting (APS/URSI), IEEE, Singapore, Singapore, Dec. 2021, pp. 1909–1910, doi:10.1109/APS/URSI47566.2021.9704198.

[37] D. Samantaray, S. Bhattacharyya, K.V. Srinivas, Modified Fractal-shaped Slotted Patch Antenna with Dipole-shaped Slotted Ground Plane with Enhanced Gain for X-band Applications, in: 2018 IEEE Indian Conference on Antennas and Propogation (InCAP), IEEE, Hyderabad, India, Dec. 2018, pp. 1–4, doi:10.1109/INCAP.2018.8770817.

[38] F. Alimenti, P. Mezzanotte, M. Dionigi, M. Virili, L. Roselli, Microwave Circuits in Paper Substrates Exploiting Conductive Adhesive Tapes, IEEE Microw. Wirel. Compon. Lett. 22 (12) (Dec. 2012) 660–662, doi:10.1109/LMWC.2012.2227141.

[39] N. Chahat, M. Zhadobov, S.A. Muhammad, L.Le Coq, R. Sauleau, 60-GHz Textile Antenna Array for Body-Centric Communications, IEEE Trans. Antennas Propag. 61 (4) (Apr. 2013) 1816–1824, doi:10.1109/TAP.2012.2232633.

[40] F. Alimenti, et al., A 24-GHz Front-End Integrated on a Multilayer Cellulose-Based Substrate for Doppler Radar Sensors, Sensors 17 (9) (Sep. 2017) 2090, doi:10.3390/s17092090.

[41] M. Poggiani, et al., 24-GHz Patch antenna array on cellulose-based materials for green wireless internet applications, IET Sci. Meas. Technol. 8 (6) (Nov. 2014) 342–349, doi:10.1049/iet-smt.2013.0279.

[42] F. Alimenti, et al., 24 GHz Single-Balanced Diode Mixer Exploiting Cellulose-Based Materials, IEEE Microw. Wirel. Compon. Lett. 23 (11) (Nov. 2013) Art. no. 11, doi:10.1109/LMWC.2013.2279125.

[43] A. Sid, P.Y. Cresson, N. Joly, F. Braud, T. Lasri, A flexible and wearable dual band bio-based antenna for WBAN applications, AEU - Int. J. Electron. Commun. (Sep. 2022) 154412, doi:10.1016/j.aeue.2022.154412.